

Enhancing Robustness in Post-Processing Watermarking: An Ensemble Attack Network Using CNNs and Transformers

Tzuhsuan Huang*
Academia Sinica
Taipei, Taiwan
jason890425@citi.sinica.edu.tw

Cheng Yu Yeo*
National Yang Ming Chiao Tung
University
Hsinchu, Taiwan
boyeyo123.ee12@nycu.edu.tw

Tsai-Ling Huang
National Yang Ming Chiao Tung
University
Hsinchu, Taiwan
christina.ii12@nycu.edu.tw

Hong-Han Shuai
National Yang Ming Chiao Tung
University
Hsinchu, Taiwan
hhshuai@nycu.edu.tw

Wen-Huang Cheng
National Taiwan University
Taipei, Taiwan
wenhuang@csie.ntu.edu.tw

Jun-Cheng Chen
Academia Sinica
Taipei, Taiwan
pullpull@citi.sinica.edu.tw

ABSTRACT

Recent studies on deep watermarking have predominantly focused on in-processing watermarking, which integrates the watermarking process into image generation. However, post-processing watermarking, which embeds watermarks after image generation, offers more flexibility. It can be applied to outputs from any generative model (e.g. GANs, diffusion models) without needing access to the model's internal structure. It also allows users to embed unique watermarks into individual images. Therefore, this study focuses on post-processing watermarking and enhances its robustness by incorporating an ensemble attack network during training. We construct various versions of attack networks using CNN and Transformer in both spatial and frequency domains to investigate how each combination influences the robustness of the watermarking model. Our results demonstrate that combining a CNN-based attack network in the spatial domain with a Transformer-based attack network in the frequency domain yields the highest robustness in watermarking models. Extensive evaluation on the WAVES benchmark, using average bit accuracy as the metric, demonstrates that our ensemble attack network significantly enhances the robustness of baseline watermarking methods under various stress tests. In particular, for the Regeneration Attack defined in WAVES, our method improves StegaStamp by 18.743%. The code is released at <https://github.com/aiiu-lab/DeepRobustWatermark>.

CCS CONCEPTS

• Security and privacy → Software and application security.

*Both authors contributed equally to this research.

Permission to make digital or hard copies of all or part of this work for personal or classroom use is granted without fee provided that copies are not made or distributed for profit or commercial advantage and that copies bear this notice and the full citation on the first page. Copyrights for components of this work owned by others than the author(s) must be honored. Abstracting with credit is permitted. To copy otherwise, or republish, to post on servers or to redistribute to lists, requires prior specific permission and/or a fee. Request permissions from permissions@acm.org.

AISEC' 25, October 17, 2025, Taipei, Taiwan

© 2025 Copyright held by the owner/author(s). Publication rights licensed to ACM.

ACM ISBN 978-1-4503-XXXX-X/2018/06...\$15.00

<https://doi.org/XXXXXXX.XXXXXXX>

KEYWORDS

Deep Watermarking; Copyright Protection; Ensemble Model

ACM Reference Format:

Tzuhsuan Huang, Cheng Yu Yeo, Tsai-Ling Huang, Hong-Han Shuai, Wen-Huang Cheng, and Jun-Cheng Chen. 2025. Enhancing Robustness in Post-Processing Watermarking: An Ensemble Attack Network Using CNNs and Transformers. In *Proceedings of the 2025 Workshop on Artificial Intelligence and Security (AISEC '25)*, October 17 2025, Taipei, Taiwan. ACM, New York, NY, USA, 11 pages. <https://doi.org/XXXXXXX.XXXXXXX>

1 INTRODUCTION

Image generation and manipulation have advanced rapidly in recent years, mainly driven by breakthroughs in generative adversarial networks (GANs) [3–12] and diffusion models [13–16]. However, with these advances, concerns over intellectual property and copyright infringement have come to the forefront, highlighting the growing importance of robust and reliable watermarking techniques.

Previous watermarking methods can be broadly categorized into post-processing and in-processing approaches. Post-processing methods embed watermarks after image generation, whereas in-processing methods integrate watermarking directly into the image generation process. In this work, we focus on post-processing techniques, which typically consist of a watermark encoder and a decoder. The encoder embeds watermarks into images, while the decoder is responsible for extracting the embedded watermarks. To improve the resilience of watermarks against noise during transmission, Zhu *et al.* [17] incorporate a noise layer, also known as attack network, to simulate common distortions occurring during image transmissions and malicious attacks. Although the noise layer greatly improves the tolerance of the watermarking model against expected distortions that are simulated during training, it is insufficient when handling unforeseen distortions. To address this limitation, Luo *et al.* [2] propose a CNN-based attack network that generates a diverse range of image perturbations, enhancing the robustness of the watermarking model to a wider range of distortions. However, we find that complex distortions (e.g. JPEG compression) are difficult to simulate using the CNN-based attack network, which limits the ability of the watermarking model to generalize to more challenging scenarios.

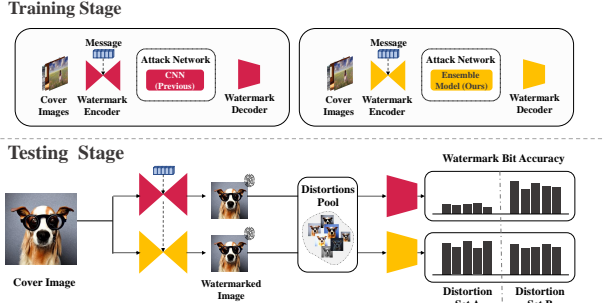


Figure 1: The CNN-based attack network proposed in “Distortion Agnostic Deep Watermarking (DA)” [2] tends to generate limited types of distortions due to its architectural capacity, which results in suboptimal performance of the watermarking model when facing unseen attacks. To overcome this limitation, we propose an ensemble attack network (ensemble model) that integrates CNN and Transformer architectures across both spatial and frequency domains to simulate a broader spectrum of attacks, thereby improving the robustness of the watermarking model. Note that the watermarking model trained with a CNN is shown in red, while the one trained with the ensemble model is shown in orange.

This limitation motivates us to adopt a Transformer-based architecture as the backbone of the attack network. While this approach substantially improves the robustness of the watermarking model, it also leads the image encoder to produce watermarked images with noticeable artifacts. This occurs because the watermark encoder must embed stronger watermarks to resist the intense perturbations introduced by the Transformer-based attack network. This observation encourages us to explore attack networks operating beyond the spatial domain. In contrast to spatial-domain perturbations that directly alter pixel intensities and often produce visible artifacts, frequency-domain modifications, particularly those based on the 2D Discrete Cosine Transform (DCT), operate in a more organized and perceptually coherent domain. Consequently, we integrate the DCT process with the Transformer architecture (DCT-Transformer) to apply distortions in the frequency domain. This approach preserves the quality of the encoded images while enhancing the model’s resilience against a wider variety of distortions.

Moreover, we find that CNN-based and DCT-Transformer-based attack networks simulate distinct types of distortion, which motivates us to employ an ensemble technique to construct attack networks in different configurations (e.g. model cascade or parallel as described in Section 3.4). Our experiments demonstrate that utilizing an ensemble model can harness the advantages of both CNN and Transformer under different domains, as shown in Figure 1, enhancing robustness of watermarks under several distortions.

To demonstrate the efficacy of the proposed ensemble attack network, we train several watermarking models using our attack network and evaluate their robustness across a wide range of attacks. Following the WAVES benchmark [18], we apply three attacks (distortion, embedding, and regeneration) defined in WAVES to evaluate the robustness of the watermarking models. In addition, we utilize off-the-shelf image editing models to attack (manipulate) watermarked images and assess whether the watermarks remain

after editing. **(1) Distortion Attacks (WAVES):** We assess the resilience of the watermarks by applying a comprehensive set of distortions that simulate realistic transmission and image processing scenarios. By integrating our ensemble attack network, we significantly enhance the robustness of baseline watermarking methods, including HiDDeN [17], StegaStamp [19], and Stable Signature [20], achieving average bit accuracy improvements of 6.995%, 5.395%, and 8.386%, respectively. **(2) Embedding Attacks (WAVES):** Against embedding attacks that utilize off-the-shelf embedding models to fool the watermark decoder, our method achieves nearly 100% bit accuracy on HiDDeN and StegaStamp, and 90.078% on Stable Signature. **(3) Regeneration Attacks (WAVES):** In regeneration attacks, we employ diffusion models or VAEs to alter the image’s latent representation. Our approach outperforms “Distortion Agnostic Deep Watermarking (DA)” and StegaStamp by 3.537% and 18.743%, respectively, while achieving performance comparable to Stable Signature. All experiments mentioned above are conducted on the COCO dataset. For **(4) Manipulation Attacks:** Our method defeats DA and StegaStamp by 9.963% and 7.551% in average bit accuracy on the COCO and CelebA datasets.

Our main contributions are twofold: (1) We present a comprehensive study on the robustness of watermarking models trained with different attack networks. Specifically, we propose using Transformer architectures as alternatives to CNNs for simulating adversarial distortions and observe that they generate distinct types of distortions. Moreover, we introduce frequency-domain perturbations by incorporating DCT processing into both CNN- and Transformer-based architectures, providing a complementary perspective to spatial-domain attacks. (2) We propose a novel ensemble attack network that combines a CNN-based attack network operating in the spatial domain with a Transformer-based attack network operating in the frequency domain. We demonstrate that this ensemble technique significantly improves the robustness of several baseline watermarking methods, as evaluated on the WAVES benchmark.

2 RELATED WORK

In this section, we briefly review the recent developments in deep learning-based image watermarking approaches [2, 17, 19, 39–43]. Following WAVES benchmark [18], current research on deep watermarking can be divided into two categories: (1) post-processing watermarking and (2) in-processing watermarking.

2.1 Post-Processing Watermarking

In general, post-processing watermarking employs deep learning techniques to embed information into generated or existing images using an encoder–decoder framework. The encoder embeds a sequence of binary messages or secret images (watermarks) into a cover image, allowing the decoder to recover the embedded message even if the watermarked image is degraded. HiDDeN [17] was the first method to adopt this end-to-end framework for watermarking. To handle distortions introduced during digital transmission, Zhu *et al.* [17] introduce a noise layer to simulate a range of transformations during training, forcing the model to learn watermark encodings that can survive such distortions. However, this approach has a significant limitation, as it requires the noise layer

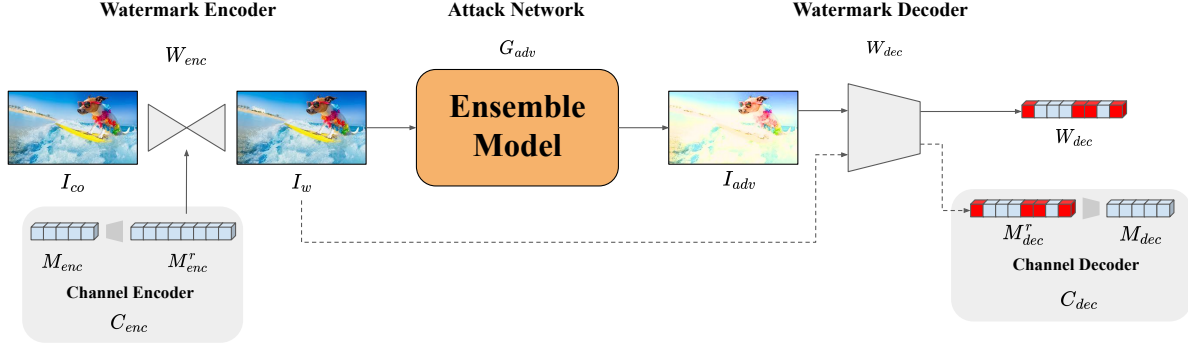


Figure 2: Our framework begins with the channel encoder C_{enc} , which injects redundancy into the encoded message M_{enc} and produces a redundant message M_{enc}^r . The watermark encoder W_{enc} then embeds M_{enc}^r into the cover image I_{co} to create the watermarked image I_w . The attack network G_{adv} generates an adversarial image I_{adv} from I_w , simulating potential transmission or processing distortions. The watermark decoder W_{dec} extracts redundant decoded messages M_{dec}^r and M_{adv}^r from I_w and I_{adv} , which are then sent to the channel decoder C_{dec} to convert them back to the decoded message M_{dec} .

to be differentiable. In practice, many common distortion operations are non-differentiable, making it impractical to incorporate them within the noise layer. To address these limitations, Fang *et al.* [32] propose a mask-guided frequency enhancement algorithm to improve the watermarking network, enhancing its robustness against practical distortions. Inheriting the concept of HiDDeN, Luo *et al.* [2] replace the noise layer with the CNN-based attack network with adversarial training to cover both known and unseen distortions. They also leverage channel coding to further enhance the robustness of watermarks. In StegaStamp [19], Tancik *et al.* propose an encoder-decoder framework that enables hyperlinks embedded in images to remain intact even after physical transmission. Although StegaStamp is highly robust to distortions that occur during image transmission in the wild, it has a relatively low capacity for embedding information. To break this restriction, Lu *et al.* [21] adopt DWT transform and Inverse DWT (IDWT) transform as down-sampling and up-sampling layers used in watermarking process to improve the performance of StegaStamp. To achieve watermark robustness against print-camera (P-C) noise, Qin *et al.* [33] designed a deep noise simulation network to simulate the fusion of real P-C noises, enhancing the robustness of the watermark.

2.2 In-Processing Watermarking

In-processing watermarking integrates watermark embedding into the image generation process. “Artificial Fingerprinting for Generative Models (AF)” [22] is the first work to investigate the transferability of watermarks in generative models. Yu *et al.* [22] embed watermarks into the training data and then use the watermarked data to train GANs, assessing whether GAN can generate images that retain the embedded watermarks. They demonstrate that their watermarking solution can be applied to a variety of generative models and ensure the robustness of the watermarks. However, the robustness of the watermarks is insufficient to withstand certain attacks. Recent approaches have focused on integrating watermark embedding into diffusion models (DMs), further enhancing watermark robustness. In “A Recipe for Watermarking Diffusion Models (Recipe)” [23], Zhao *et al.* undertake a thorough investigation for

customizing traditional watermarking methods to effectively integrate watermarking process into cutting-edge DMs, such as Stable Diffusion [24]. Fernandez *et al.* [20] fine-tune the VAE decoder within the latent diffusion models to generate images containing predefined watermarks. Wen *et al.* [25] embed the watermarks into the latent noise of DMs under frequency domain, making watermarks more resistant to removal by malicious users. Lukas *et al.* [27] fine-tune the generative model, using model’s prior knowledge and a well-trained watermark decoder to produce watermarked images. Kim *et al.* [26] introduce a weight modulation process, enabling the model to embed various watermarks into generated images rather than being limited to a single predefined one.

In our experiments, we demonstrate that the proposed method improves the robustness of post-processing watermarking models. We further show that it also enhances the robustness of Stable Signature [20], an in-processing watermarking method.

3 THE PROPOSED METHOD

In Section 3.1, we introduce the previous watermarking pipeline, including the overall framework and the objective loss used to train the model. Section 3.2 highlights the limitations of the attack network (CNN) employed in “Distortion Agnostic Deep Watermarking (DA)” [2] and presents a new Transformer-based alternative. In Section 3.3, we assess the effectiveness of different architectures in both the spatial and frequency domains, providing detailed explanations and results. Finally, Section 3.4 explores various ensemble techniques aimed at combining the strengths of different attack networks under multiple configurations.

3.1 Preliminaries

To evaluate the efficacy of our attack network, we integrate it into two state-of-the-art (SOTA) post-processing watermarking methods: HiDDeN [17] and StegaStamp [19]. Following DA [2], we incorporate channel coding (NECST) [1] into the watermarking pipeline of HiDDeN. As illustrated in Figure 2, the pipeline consists of three components: a channel coding model, a watermarking model, and

Table 1: We calculate the bit accuracy between encoded and decoded watermarks, evaluating them under various distortions as defined in WAVES [18]. “Methods” and “Trans” indicate different attack networks and Transformer, respectively. The CNN mentioned here is our re-implementation of “Distortion Agnostic Deep Watermarking (DA)” [2], as the authors, Luo *et al.* [2], did not release their code and pre-trained weights. All networks are trained and evaluated on the COCO dataset. The parameter p represents the strength of the distortion; for instance, in the resizedcrop attack, 10% to 15% of the watermarked image is cropped before being sent to the decoder to extract the watermarks. The highest score is highlighted in bold. Note that the CNN performs best on red-marked distortions, while the DCT-Transformer performs best on blue-marked distortions.

Methods	Identity	resizedcrop $p = 10 \sim 15\%$	erasing $p = 5 \sim 25\%$	brightness $p = 20 \sim 100\%$	blurring $p = 4 \sim 20pix$	rotation $p = 9^\circ \sim 45^\circ$	contrast $p = 20 \sim 100\%$	noise $std = 0.02 \sim 0.1$	compression $p = 90 \sim 10$	Avg
(a) CNN [2]	99.947	90.301	99.1	97.917	49.991	52.699	97.852	58.793	68.423	79.447
Trans	97.472	64.596	95.383	92.018	53.038	59.935	92.786	91.348	90.828	81.933
(b) DCT-CNN	99.294	74.366	96.579	94.563	50.141	54.508	95.003	77.131	79.014	80.066
DCT-Trans	99.678	86.824	93.965	97.799	49.909	58.046	98.234	95.772	93.007	85.914

an attack network. The channel coding model is composed of a channel encoder C_{enc} and a decoder C_{dec} . The watermarking model is composed of a watermarking encoder W_{enc} and a watermarking decoder W_{dec} . The attack network G_{adv} in HiDDeN is composed of several pre-defined noises including Crop, Gaussian Blur, etc. The training pipeline can be divided into the following three parts.

Channel Coding. The objective loss used to train channel coding model is shown below

$$\mathcal{L}_C(\theta_{NECST}) = -\frac{1}{L_M} \sum_{i=0}^{L_M} M_i \cdot \log(\sigma(\hat{M}_i)) + (1 - M_i) \cdot \log(1 - \sigma(\hat{M}_i)), \quad (1)$$

where θ_{NECST} denotes the parameters of the channel coding model, L_M is the length of the original binary message M_i , and \hat{M}_i is the recovered message from the NECST model. The function σ represents the sigmoid function. Note that the NECST model is optimized independently of the watermarking model.

Watermarking Models. The watermark encoder W_{enc} is optimized using the objective loss shown below

$$\mathcal{L}_E(\theta_{W_{enc}}) = \alpha_{W_{enc}}^1 \|I_{co} - I_w\|^2 + \alpha_{W_{enc}}^2 \mathcal{L}_G(I_w), \quad (2)$$

where $\alpha_{W_{enc}}^1, \alpha_{W_{enc}}^2$ are hyperparameters for the loss function, and I_{co}, I_w refer to the cover image and the watermarked image, respectively. The GAN loss \mathcal{L}_G is employed to enhance the quality of watermarked images by jointly training a discriminator, which aims to minimize the perceptible differences between the cover and watermarked images. This ensures that the modifications introduced during the watermarking process are virtually undetectable.

The watermarking decoder W_{dec} is optimized using the objective loss shown below

$$\mathcal{L}_D(\theta_{W_{dec}}) = \alpha_{W_{dec}}^1 \|M_{dec}^r - M_{enc}^r\|^2 + \alpha_{W_{dec}}^2 \|M_{adv}^r - M_{enc}^r\|^2, \quad (3)$$

where $\alpha_{W_{dec}}^1, \alpha_{W_{dec}}^2$ are hyperparameters for the loss function, and $M_{dec}^r, M_{enc}^r, M_{adv}^r$ refer to the redundant decoded messages, redundant encoded messages (watermarks after channel coding), and redundant adversarial decoded messages, respectively. The watermark decoder is optimized by minimizing the mean squared error between the original messages (watermarks) and the decoded messages from both watermarked and adversarial images.

Attack Network. The attack network G_{adv} aims to generate distortions that can enhance the robustness of the watermarking model. The objective loss for the attack network is shown below

$$\mathcal{L}_{adv}(\theta_{G_{adv}}) = \alpha_{adv}^1 \|I_{adv} - I_w\|^2 - \alpha_{adv}^2 \|M_{adv}^r - M_{enc}^r\|^2, \quad (4)$$

where $\alpha_{adv}^1, \alpha_{adv}^2$ are hyperparameters for the loss function, and I_{adv}, I_w refer to adversarial images and watermarked images, respectively. The coefficient α_{adv}^1 encourages the minimization of differences between the watermarked and adversarial images, while α_{adv}^2 guides the attack network to generate adversarial examples by injecting noise into the watermarked images.

In StegaStamp, the training pipeline follows a similar structure, with the key difference being the absence of a channel coding.

In this work, we focus on analyzing the influence of different attack networks on the robustness of watermarking models. The comparison of different architectures and domains is provided in the following sections.

3.2 Analysis of CNN and Transformer

Although it has been demonstrated that a CNN-based attack network [2] can effectively improve the performance of the watermarking models through adversarial training, there is still an imperfection in robustness for certain complex distortions (e.g. JPEG compression). Our analysis indicates that the limitation of the CNN architecture stems from its restricted kernel size and receptive field. Despite this limitation can be alleviated by stacking more layers into the CNN model to expand the receptive field, Luo *et al.* [2] mention that an increase in model complexity can lead to a decrease in the robustness of watermarks. To solve this problem, we investigate a Transformer architecture as a potential solution. To employ the Transformer as the model backbone in adversarial training, the watermarked image is first divided into 8×8 image patches and projected into patch embedding tokens. These tokens are then processed by the Transformer via the multi-head self-attention:

$$\text{Multihead}(X_e) = \text{Concat}_{i=1}^m \left\{ \text{softmax} \left(\frac{W_i^Q X_e (W_i^K X_e)^T}{\sqrt{d_K}} \right) W_i^V X_e \right\}, \quad (5)$$

where d_K is the dimensionality of the key vectors and **Concat** denotes the concatenation operation with m heads, X_e represents the input embedding tokens, and W_i^Q, W_i^K, W_i^V are trainable matrices of weight parameters that transform features from X_e to get the query, key, and value matrices respectively.

Although the Transformer-based attack network improves watermark robustness, as shown in Table 1(a), it also reduces the *Identity value*, which measures decoding ability on clean (undistorted) watermarked images. A low Identity value means the decoder cannot

Table 2: This table illustrates the impact of varying α_{adv}^2 on the Identity value of the watermarking model.

Methods	0.02	1.0	5.0	7.5
DCT-Trans	99.953	99.477	72.517	71.471
Trans	98.345	96.905	54.551	59.651

reliably extract the watermark even without any distortions, making the model impractical. This suggests that while strong spatial-domain distortions enhance robustness against many attacks, they can also interfere with the model's basic decoding ability. To mitigate this issue, we investigate attack networks that operate in the frequency domain, which can simulate challenging distortions while better preserving the Identity value.

3.3 Analysis of Spatial and Frequency Domains

First of all, we argue that the adversarial loss function (4) for the attack network is incompatible, as it is difficult to inject perturbations in the spatial domain while maintaining the quality of watermarked images, which in turn reduces the accuracy of recovering the embedded watermark from encoded images (Identity value). Our experiment shows that if the adversarial images are highly distorted due to the second term in Eq. (4), it is hard for the watermarking model to converge during training. As shown in Table 2, the Identity value decreases significantly as α_{adv}^2 increases. This suggests that to facilitate the convergence of the watermarking model, reducing the strength of the distortion is necessary. However, such reduction in distortion strength inevitably leads to a decrease in the robustness of watermarks against distortions. This inspires us to investigate the attack network's ability to generate adversarial images in the frequency domain.

Unlike spatial-domain perturbations that directly alter pixel intensities and often introduce visible artifacts, frequency-domain perturbations (e.g. via 2D-DCT) offer a more perceptually aware and structured space. The DCT separates image content by frequency, with low-frequency coefficients encoding global structure and high-frequency ones capturing fine details. This allows us to introduce distortions into selected bands that are more vulnerable to attacks but less perceptible to the human eye. Prior work [44, 45] has shown that DCT attacks achieve a better trade-off between invisibility and attack effectiveness. By operating in the DCT domain, we improve the robustness of the watermark while preserving visual quality and training stability. The forward 2D-DCT is computed with the formula given by

$$X_{i,j} = \frac{1}{\sqrt{2N}} k(i)k(j) \sum_{x=0}^{N-1} \sum_{y=0}^{N-1} I_{x,y} \cos \left[\frac{(2x+1)i\pi}{2N} \right] \cos \left[\frac{(2y+1)j\pi}{2N} \right], \quad (6)$$

where $k(i)$, $k(j)$ are the normalizing factors, $I_{x,y}$ is the pixel value at location (x, y) and $X_{i,j}$ is the DCT coefficient at (i, j) . To integrate the DCT with an adversarial attack network, our first step involves refining the watermarked image in the YUV color space, followed by computing the forward 2D-block-DCT on each 8×8 non-overlapping block of the watermarked image. Next, we selectively mask the high-frequency components of the DCT coefficients

Algorithm 1 Integration of the DCT-Process

Input: Watermarked Images I_w , Attack Network G_{adv} ;

Output: Adversarial Images I_{adv} ;

Convert color space of I_w from RGB to YUV;

Apply 2D-block-DCT on each non-overlapping 8×8 block of I_w to get DCT representation I_w^{DCT} ;

Apply high frequency mask on each block of I_w^{DCT} ;

if $G_{adv} \in$ Transformer **then**

Split I_w^{DCT} into 8×8 blocks;

Rearranging DCT coefficients by frequency band across blocks;

end if

$I_{adv}^{DCT} = G_{adv}(I_w^{DCT})$;

Apply 2D-IDCT on I_{adv}^{DCT} to get I_{adv} ;

Convert the color space of I_{adv} from YUV back to RGB;

return I_{adv} ;

for each YUV channel while preserving the remaining parts to apply perturbations. Then, the intermediate DCT representation of the watermarked image is passed through the Transformer or CNN. Finally, the procedure ends with applying the inverse DCT to obtain the output followed by converting it back to the RGB color space from the YUV color space. Additionally, since we hope to fully utilize the potential of the self-attention mechanism in the Transformer, there is a minor difference in procedure between CNN and the Transformer. Specifically, before passing the intermediate DCT representation through Transformer, we divide the intermediate DCT representation into 8×8 pixel blocks. Afterward, we rearrange them in the order of frequency bands (we put the DCT coefficients of the same frequency band from different blocks together) and then pass them through the Transformer. We demonstrate the detailed procedures for integrating the DCT process into both CNN-based and Transformer-based attack networks in Algorithm 1. As illustrated in Table 1(b), the application of DCT markedly enhances the performance of the Transformer-based method. However, the CNN-based attack network shows limited improvement, primarily due to its restricted receptive field, which prevents it from effectively capturing signal correlations across different frequencies.

To avoid naming confusion, in the following sections, "DCT-CNN" and "DCT-Transformer" refer to the CNN- and Transformer-based attack networks integrated with the DCT process. The original CNN-based and Transformer-based attack networks are referred to as "CNN" and "Transformer", respectively.

3.4 Ensemble Models

By comparing the performance of watermarking models trained with CNN and DCT-Transformer, as shown in Table 1, we observe that each watermarking model excels under different types of distortions. To enhance the robustness of the watermarking model against diverse distortions, we explore the combination of CNN and DCT-Transformer in four configurations: *Model Cascade*, *Model Parallel*, *Aggregate Blend*, and *Random Blend*. The detailed procedures of these four ensemble methods are illustrated in Figure 3.

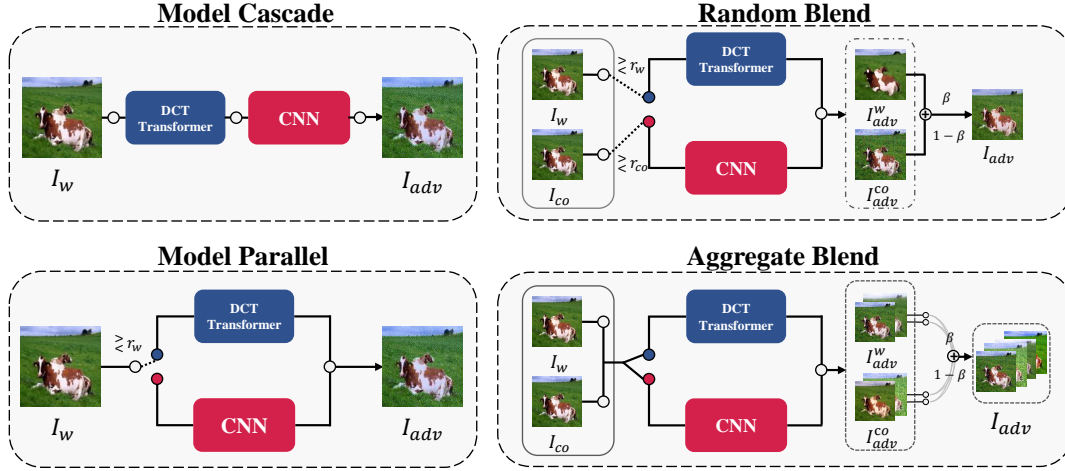


Figure 3: The illustration of four distinct configurations of ensemble methods, including Model Cascade, Model Parallel, Random Blend, and Aggregate Blend. These methods employ various strategies to generate adversarial images I_{adv} from watermarked images I_w and cover images I_{co} .

Table 3: All evaluation settings remain identical to those outlined in Table 1. This table displays the decoded watermark accuracy for ensemble models, including Model Cascade, Model Parallel, Random Blend, and Aggregate Blend. Each ensemble model consists of different configurations combining the DCT-Transformer with the CNN.

Methods	Identity	resizedcrop $p = 10 \sim 15\%$	erasing $p = 5 \sim 25\%$	brightness $p = 20 \sim 100\%$	blurring $p = 4 \sim 20pix$	rotation $p = 9^\circ \sim 45^\circ$	contrast $p = 20 \sim 100\%$	noise $std = 0.02 \sim 0.1$	compression $p = 90 \sim 10$	Avg
Model Cascade	99.947	87.573	98.452	98.026	49.859	52.338	98.268	92.898	87.236	84.955
Model Parallel	99.851	86.28	99.364	99.448	50.378	54.178	99.024	96.464	92.997	86.442
Random Blend	99.976	85.896	99.807	98.437	50.092	44.992	99.324	91.174	86.377	84.008
Aggregate Blend	99.984	85.558	99.713	98.787	49.99	48.574	99.257	87	86.634	83.944

Model Cascade. During each iteration of the training process, the watermarked image I_w is initially passed through the DCT-Transformer, and then forwarded to CNN for distortion generation.

Model Parallel. In this dual-path setup, the watermarked image I_w is randomly passed through either the DCT-Transformer or the CNN based on a predetermined threshold r_w . For each iteration, a random value in the interval $[0,1]$ is generated. If the value exceeds the threshold r_w , the watermarked image I_w will be processed by the DCT-Transformer; otherwise, it is passed through the CNN.

Random Blend. To preserve the original pixel information, both the cover image I_{co} and the watermarked image I_w are used as inputs to the attack network. For each image, a random threshold r_{co} for I_{co} and r_w for I_w is used to decide whether it will be processed by the DCT-Transformer or the CNN. Importantly, in each iteration, exactly one of the two images is passed through the DCT-Transformer and the other through the CNN, ensuring a complementary processing path. After generating I_{adv}^{co} and I_{adv}^w , the two outputs are blended using a blending factor β according to the equation $I_{adv} = \beta \cdot I_{adv}^w + (1 - \beta) \cdot I_{adv}^{co}$, where $\beta \in [0, 1]$ is randomly generated in each iteration.

Aggregate Blend. In contrast to the Random Blend method, both the cover image I_{co} and the watermarked image I_w are passed through the DCT-Transformer and the CNN, resulting in two sets

of adversarial images, I_{adv}^{co} and I_{adv}^w , each containing two adversarial images. We randomly select one image from each sets and blend the selected images together using a blending coefficient β . Consequently, the final adversarial output I_{adv} is an aggregation of many possible combinations.

Among four ensemble strategies, Model Parallel (MP) attains the highest average bit accuracy, as shown in Table 3, suggesting that balanced exposure to diverse distortions helps prevent overfitting to any single distortion characteristic and thereby improves overall robustness. This hypothesis is further supported by the observation that the performance of the watermarking model trained with Model Parallel (MP) generally lies between those trained exclusively with CNN or DCT-Transformer attack networks. For instance, it outperforms the CNN in handling compression distortions while remaining comparable to the DCT-Transformer. These findings are further validated by comparisons under various distortion levels, as illustrated in Figure 4.

4 EXPERIMENTS

We first provide detailed descriptions of the experimental settings in Section 4.1, and then demonstrate the improvement in watermark robustness achieved by applying the proposed ensemble network to state-of-the-art (SOTA) post-processing watermarking models in

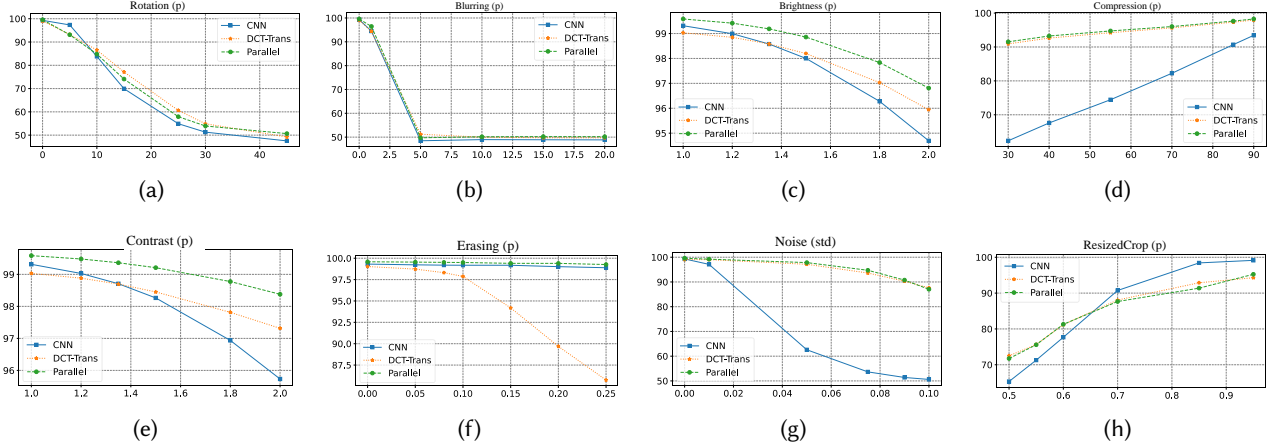


Figure 4: We compare the bit accuracy (y-axis) of different watermarking models trained with distinct attack networks. The proposed ensemble method, which integrates CNN and DCT-Transformer attack networks, achieves performance comparable to models trained with either CNN or DCT-Transformer alone across all distortion parameters (x-axis, shown as p or std depending on the attack). This demonstrates that our method effectively combines the strengths of both architectures.

Table 4: All training settings remain identical to those outlined in Table 1. HiDDeN_MP refers to the use of Model Parallel as an attack network, jointly trained with HiDDeN’s encoder-decoder network, and the same applies to StegaStamp_MP. Notably, HiDDeN is a re-implemented version in PyTorch, as Zhu *et al.* [17] only provided a TensorFlow version.

Methods	Dataset	Identity	resizedcrop $p = 10 \sim 15\%$	erasing $p = 5 \sim 25\%$	brightness $p = 20 \sim 100\%$	blurring $p = 4 \sim 20\text{pix}$	rotation $p = 9^\circ \sim 45^\circ$	contrast $p = 20 \sim 100\%$	noise $std = 0.02 \sim 0.1$	compression $p = 90 \sim 10$	Avg
HiDDeN [17]	COCO	99.11	84.479	98.547	96.806	51.314	56.706	97.699	55.957	57.108	77.525
DA [2]	COCO	99.947	90.301	99.1	97.917	49.991	52.699	97.852	58.793	68.423	79.447
StegaStamp [19]	COCO	99.999	48.265	99.564	98.521	49.897	49.994	99.012	89.359	50.866	76.164
HiDDeN_MP (ours)	COCO	99.851	86.28	99.364	99.448	50.378	54.178	99.024	96.464	92.997	86.442
StegaStamp_MP (ours)	COCO	99.999	50.509	96.396	95.073	50.384	50.263	97.17	95.264	98.981	81.559
HiDDeN	CelebA	99.092	84.833	98.231	96.212	51.242	57.426	96.492	52.438	55.293	76.806
DA	CelebA	99.99	90.964	98.958	97.719	49.908	53.185	97.562	54.291	63.859	78.492
StegaStamp	CelebA	99.99	47.842	99.669	98.883	49.853	50.012	98.897	88.784	51.052	76.109
HiDDeN_MP (Ours)	CelebA	99.592	86.045	98.864	97.787	50.422	53.959	98.287	95.451	91.878	85.809
StegaStamp_MP (Ours)	CelebA	99.999	50.341	96.381	94.541	50.203	50.008	95.511	94.47	98.916	81.152

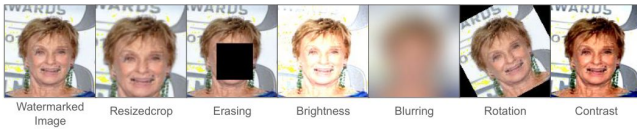


Figure 5: We show the watermarked images after being subjected to the distortions utilized in the evaluation.

Section 4.2. Finally, in Section 4.3, we show that the enhanced post-processing model can also benefit the in-processing watermarking method Stable Signature [20].

4.1 Experimental Settings

For evaluation, we compute the bit accuracy between encoded and extracted watermarks to assess their robustness in various scenarios. We use the watermark stress tests defined in WAVES [18] to evaluate the resistance of watermarks against **Distortion Attacks**, **Embedding Attacks**, and **Regeneration Attacks** in both post-processing and in-processing watermark experiments. In **Manipulation Attacks**, we evaluate watermark robustness after manipulations made by SOTA image editing models in the post-processing watermark experiment. To ensure both robustness and imperceptibility, we

also measure the quality of watermarked images using Peak Signal-to-Noise Ratio (PSNR) and Structural Similarity Index (SSIM).

Implementation Details. We train the models on the COCO [31] dataset and evaluate their performance on both the COCO and CelebA [30] datasets. Following recent works, we resize the images to 128×128 pixels for training and evaluation. In the COCO dataset, the training set comprises 110k images, and the testing set comprises 40k images. For the CelebA dataset, the training set consists of 150k images, and the testing set comprises 50k images. The channel coding model follows the design used in DA [2], where the original 30-bit message (watermark) is expanded to 120 bits using the NECST [1] model to inject noise redundancy. The Transformer attack network adopts the standard encoder architecture from ViT [28]. Specifically, the cover image is split into 8×8 patches and projected into embeddings with 256 dimensions. The number of encoder layers is $D = 6$, and attention heads $H = 12$ are chosen to optimize the training process. For the Transformer attack network, we set the learning rate to $1e - 4$ and the weight decay to $1e - 3$. For the CNN attack network, the watermarking components (e.g., Encoder, Decoder, Discriminator), and the loss function hyperparameters, we follow the same settings as DA [2]. The learning rate

Table 5: Comparison of watermarked image quality between our method and previous approaches.

Methods	RGB	Y	PSNR \uparrow			SSIM \uparrow
			U	V	B	
HiDDeN [17]	33.463	34.701	40.91	37.977	33.079	0.964
DA [2]	34.559	35.23	45.26	45.185	33.877	0.969
StegaStamp [19]	45.9	50.084	51.309	47.764	42.062	0.995
HiDDeN_MP (Ours)	31.062	31.193	42.968	39.343	30.813	0.947
StegaStamp_MP (Ours)	37.623	38.747	47.168	42.999	36.142	0.982

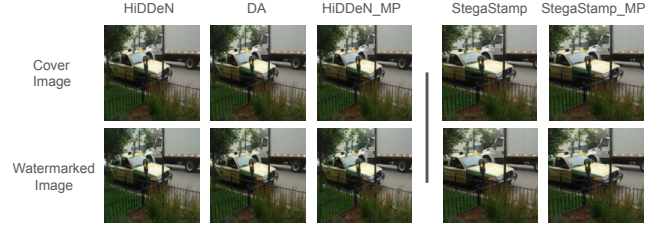
of both the CNN attack network and the watermarking components is set to 1×10^{-3} . For the loss function hyperparameters, we set $\alpha_{W_{enc}}^1 = 1.5$ and $\alpha_{W_{enc}}^2 = 0.01$ for the watermark encoder, and $\alpha_{W_{dec}}^1 = 0.3$ and $\alpha_{W_{dec}}^2 = 0.2$ for the watermark decoder. In the attack network, we set $\alpha_{adv}^1 = 15.0$ and $\alpha_{adv}^2 = 1.0$. Finally, in the ensemble methods, both thresholds r_w and r_{co} are set to 0.7.

WAVES and Manipulation Attacks. To safeguard ownership, watermarks must withstand multiple attacks during transmission or manipulation. Therefore, we utilize the benchmarks defined in WAVES [18] to assess the robustness of watermarks. **Distortion Attacks:** Watermarked images frequently experience distortions during digital transmission. However, most studies evaluate watermark robustness only in isolated or extreme cases. An *et al.* [18] set reasonable-strength distortion attacks as baseline tests for assessing the robustness of watermarks. **Embedding Attacks:** An *et al.* [18] explore whether adversarial images crafted using the PGD algorithm [34], within a perturbation limit, can cause off-the-shelf embedding models to deceive the decoder. They utilize pre-trained models such as ResNet18 [35], CLIP’s image encoder [36], KLVAE(f8), SDXL-VAE [37], and KL-VAE(f16) in this experiment. **Regeneration Attacks:** An *et al.* [18] employ diffusion models or VAE [38] to alter an image’s latent representation through a process of noising and denoising, to investigate whether watermarked images can resist these processes. Moreover, they explore the robustness of watermarks while undergoing multiple cycles of the noising and denoising process, unlike existing works focus on a single regeneration process. **Manipulation Attacks:** To test the practicality of using these watermarking models in real-world scenarios, we utilize the Diffusion-based model, InstructPix2Pix [14], to transform the style of the watermarked images into a cartoon style. For the GAN-based approach, we employ StyleRes [11] to modify watermarked images based on various prompts, such as changing hair color or altering the depicted individual’s gender.

As discussed in Section 3.4, the watermarking model trained with the Model Parallel (MP) attack network achieves the highest average bit accuracy. Therefore, in the following experiments, we compare HiDDeN [17] trained with MP (HiDDeN_MP) and StegaStamp [19] trained with MP (StegaStamp_MP) against previous methods.

4.2 Post-processing Watermarks

Distortion Attacks. We train models on COCO training set and embed watermarks in both CelebA and COCO testing sets. The watermarked images are then subjected to a range of distortions to evaluate their resilience. Subsequently, we feed the distorted watermarked images into the decoder to compute the bit accuracy

**Figure 6: We show the difference between cover images and watermarked images generated by different models.****Table 6: We evaluate previous post-processing watermarking approaches and combine them with our method to test their performance under embedding attacks.**

Methods	ResNet18	CLIP	KLVAE8	SdxlVAE	KLVAE16	Avg
HiDDeN [17]	90.089	91.322	90.77	90.881	88.005	90.213
DA [2]	93.931	95.057	95.534	95.153	92.58	94.451
StegaStamp [19]	99.876	99.319	99.934	99.883	99.874	99.777
HiDDeN_MP (Ours)	99.081	99.145	99.265	99.289	98.424	99.04
StegaStamp_MP (Ours)	99.622	99.667	99.343	99.538	97.851	99.204

Table 7: We assess previous post-processing watermarking approaches and integrate them with our method to evaluate their performance against regeneration attacks.

Methods	Regen-Diff	Regen-VAE	Regen-Diff2X	Regen-Diff4X	Avg
HiDDeN [17]	51.237	50.299	51.034	50.910	50.870
DA [2]	50.599	50.228	50.408	50.388	50.405
StegaStamp [19]	49.900	50.500	50.100	50.200	50.175
HiDDeN_MP (Ours)	56.354	50.320	55.334	53.763	53.942
StegaStamp_MP (Ours)	61.396	97.063	59.733	57.48	68.918

of the extracted watermark. As shown in Table 4, our method (HiDDeN_MP and StegaStamp_MP) outperforms DA [2] in average bit accuracy by 6.995% on COCO and 7.317% on CelebA, and improves StegaStamp [19] by 5.395% on COCO and 5.043% on CelebA. Furthermore, we show distorted images in Figure 5 to illustrate that our method can extract watermarks even when strong perturbations have severely degraded the quality of the watermarked image.

Additionally, ensuring both bit accuracy and the perceptual invisibility of watermarks is essential. Although the PSNR and SSIM values of watermarked images produced by the models trained with MP are slightly lower than those of other models (see Table 5), the images generated by our methods (HiDDeN_MP and StegaStamp_MP) still exhibit high visual quality, as shown in Figure 6.

Embedding Attacks. We calculate the bit accuracy between the encoded and extracted watermarks after attacks using five off-the-shelf embedding models. We show the experimental results in Table 6 and demonstrate that the watermark encoder-decoder jointly trained with MP achieves nearly 100% bit accuracy.

Regeneration Attacks. We evaluate the robustness of watermarks through noising and denoising process. Watermarked images are passed through DMs or VAEs [38], where they are mapped to latent representations and subsequently reconstructed. After regeneration, the images are fed into the decoder to extract the watermarks, and the bit accuracy is computed between encoded and decoded watermarks. As shown in Table 7, our method outperforms average bit accuracy by 3.537% over DA and by 18.743% over StegaStamp.

Manipulation Attacks. To assess the robustness of watermarks against image editing models, we utilize SOTA GAN-based and

Table 8: All methods are trained on the COCO dataset. After editing by generative models, we compute the bit accuracy of watermarked images in both the COCO and CelebA datasets. In the COCO dataset, we utilize InstructPix2Pix to edit the images. In the CelebA dataset, we employ StyleRes for image editing.

	COCO (InstructPix2Pix)	CelebA (StyleRes)					
Methods	Cartoon, Doodle	Smile	Glasses	Negative Gender	Overexposed	Purple Hair	Avg
HiDDeN [17]	59.841	51.299	51.58	50.993	51.355	51.127	52.699
DA [2]	69.132	59.121	59.762	56.108	60.087	59.993	60.700
Stegastamp [19]	52.142	50.040	49.957	49.948	49.992	50.004	50.347
HiDDeN_MP (Ours)	70.984	70.780	72.435	63.477	73.999	72.306	70.663
StegaStamp_MP (Ours)	77.731	53.161	54.348	53.693	54.259	54.200	57.898

Table 9: “Stable Signature MP” refers to fine-tuning VAE decoder using the enhanced watermark decoder trained with MP. We follow the training procedure outlined in Stable Signature [20] to fine-tune the VAE. Notably, the performance of Stable Signature is reproduced using a HiDDeN decoder trained by us, and the evaluation is carried out on the COCO dataset.

Methods	Identity	resizedcrop $p = 10 \sim 15\%$	erasing $p = 5 \sim 25\%$	brightness $p = 20 \sim 100\%$	blurring $p = 4 \sim 20\text{pix}$	rotation $p = 9^\circ \sim 45^\circ$	contrast $p = 20 \sim 100\%$	noise $std = 0.02 \sim 0.1$	compression $p = 90 \sim 10$	Avg
Stable Signature [20]	99.863	66.264	71.653	72.467	46.341	49.782	75.166	64.625	58.18	67.149
Stable Signature MP (Ours)	99.741	80.241	88.829	87.039	38.247	48.109	89.53	82.94	65.143	75.535

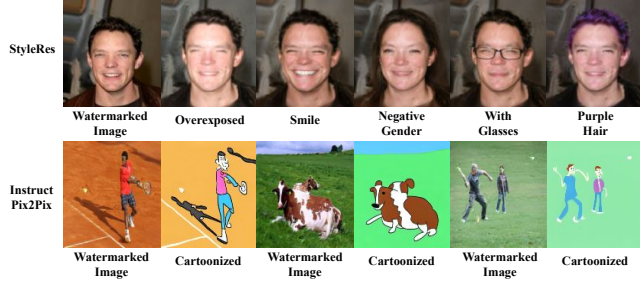


Figure 7: We utilize StyleRes [11] for editing the watermarked images embedded in CelebA with various prompts, as demonstrated in the top row. The second row showcases the outcomes of watermarked images (COCO dataset) after being edited by InstructPix2Pix [14], where we employ the prompts “cartoon, doodle” for editing the images.

diffusion-based models, StyleRes [11] and InstructPix2Pix [14], to manipulate the watermarked images using various prompts. Specifically, we embed watermarks into the CelebA testing set, which contains 50k images, and apply StyleRes to edit the images with attribute-based prompts. For example, altering gender or adding a smile. Similarly, we embed watermarks into the COCO testing set, comprising 40k images, and use InstructPix2Pix to apply edits with the prompts “Cartoon and Doodle.” Examples of the edited images are shown in Figure 7. We then input the edited images into the decoder to evaluate its ability to recover the embedded watermarks. As shown in Table 8, our method outperforms average bit accuracy by 9.963% over DA [2] and by 7.551% over StegaStamp [19].

4.3 In-processing Watermarks

Fernandez *et al.* [20] utilize a pre-trained HiDDeN decoder to fine-tune the autoencoder of latent diffusion model (LDM) [24] with a predefined watermark, guiding LDM to generate images that inherently contain the watermark. This approach allows for simultaneous image and watermark generation in a single step.

Table 10: We compare the performance of Stable Signature and our method under embedding attacks, with all evaluations performed on the COCO dataset.

Methods	ResNet18	CLIP	KLVAE8	SdxIAVE	KLVAE16	Avg
Stable Signature [20]	89.307	89.335	89.721	89.446	88.845	89.330
Stable Signature MP (Ours)	90.235	90.098	90.396	89.966	89.695	90.078

Building on the effectiveness of our proposed ensemble attack network (MP) in improving the robustness of post-processing watermarking models, we extend our evaluation to in-processing watermarking. Specifically, we fine-tune LDM using both the original HiDDeN decoder and the decoder trained with MP. After image generation, we compute the bit accuracy between the original encoded watermark and the extracted one. Notably, we use the HiDDeN model that we trained to conduct the experiments.

Distortion Attacks. We apply a series of distortions defined in WAVES [18] to attack the watermarked images and evaluate the bit accuracy of the degraded outputs. As shown in Table 9, LDM fine-tuned with decoder trained with MP outperforms the one fine-tuned with original HiDDeN decoder by 8.386% in average bit accuracy.

Embedding Attacks. We utilize five off-the-shelf embedding models to attack watermarked images generated by LDM and calculate the bit accuracy between the encoded and extracted watermarks. As shown in Table 10, the average bit accuracy achieves 90.078% by applying MP.

Regeneration Attacks. We send the generated image as input to diffusion models or VAE, mapping it to the latent space and reconstructing it. After reconstruction, we input the image into the decoder to extract the watermarks and calculate the bit accuracy between the encoded and decoded watermarks. As shown in Table 11, our method is slightly lower than Stable Signature by 0.605% while still being comparable.

5 ABLATION STUDIES

We conduct extensive ablation studies on the COCO [31] dataset to thoroughly explore the synergy between the DCT process and the

Table 11: We compare the performance of Stable Signature and our method under regeneration attacks, with all evaluations performed on the COCO dataset.

Methods	Regen-Diff	Regen-VAE	Regen-Diff2X	Regen-Diff4X	Avg
Stable Signature [20]	50.926	56.829	52.617	54.383	53.688
Stable Signature MP (Ours)	49.536	61.365	50.390	51.042	53.083

Table 12: Results of varying the number of transformer encoder blocks (Depth) and attention heads (Head) in the DCT-Transformer attack network. AVG_{ALL} denotes the average bit accuracy across all distortions that are shown in Table 1.

Transformer Configurations						
Depth	Head	params	Identity	Dropout $p = 0.3$	Sat $f = 15.0$	AVG_{ALL}
6	12	5.664M	99.678	<u>90.103</u>	84.702	85.914
12	12	11.180M	99.837	89.946	84.699	79.706
24	12	22.211M	99.958	94.405	83.648	<u>79.832</u>

Table 13: Using the same settings as Table 12, this table shows the results of the DCT-Transformer attack network with and without positional embedding.

Transformer Configurations						
Depth	Head	+ Pos emb	Identity	Dropout $p = 0.3$	Sat $f = 15.0$	AVG_{ALL}
6	12		99.678	90.103	84.702	85.914
6	12	✓	99.768	<u>89.031</u>	<u>78.565</u>	<u>80.046</u>

Table 14: Using the same settings as Table 12, this table presents the results of applying different color spaces in the DCT-Transformer attack network.

Transformer Configurations						
Depth	Head	Color Space	Identity	Dropout $p = 0.3$	Sat $f = 15.0$	AVG_{ALL}
6	12	YUV	99.678	90.103	84.702	85.914
6	12	RGB	<u>69.530</u>	<u>55.351</u>	<u>63.520</u>	<u>57.935</u>

Transformer architecture. Our investigation examines the impact of various configuration settings within the DCT-Transformer, including the number of standard Transformer encoder blocks (depth), the number of attention heads, the use of positional embeddings, and the choice of color space (YUV versus RGB).

Depth of Transformer Block. Our analysis focuses on the architecture of the Transformer-based attack network. As shown in Table 12, increasing the depth of the Transformer by adding more encoder layers does not necessarily improve performance. This is because excessive model complexity can hinder training and increase the risk of overfitting, especially when the added depth does not meaningfully enhance the model’s ability to capture relevant information in the watermarking context.

Positional Embeddings in Transformer. Positional embeddings in Transformers typically serve to provide spatial context. However, in the context of our DCT-Transformer, we find that removing positional embeddings improves performance, as shown in Table 13. This improvement can be attributed to the nature of watermarking

and attack processes, where absolute spatial positioning is less critical. Instead, capturing and manipulating frequency-based features, which are more global and resilient to common image transformations, proves to be more effective.

Color Space of DCT-Transformer. Our study also investigates the effectiveness of different color spaces, specifically evaluating the performance of the DCT process within these spaces, as shown in Table 14. The results demonstrate that the YUV color space outperforms RGB color space. This advantage is likely due to YUV’s separation of luminance (Y) and chrominance (U and V) components. The Y component, which captures brightness information, tends to retain more relevant features for watermarking and is less susceptible to distortions than the chrominance channels. By leveraging this property, applying the DCT process in the YUV color space enhances both robustness and effectiveness of the watermarking model against attacks.

6 CONCLUSIONS

We conduct a comprehensive investigation into the impact of different attack networks and ensemble strategies on watermark robustness, and propose a novel ensemble attack network to enhance the resilience of deep image watermarking pipelines. To evaluate the effectiveness of our proposed approach, we assess watermark robustness using the challenging WAVES benchmark. First, we evaluate the resilience of watermarks under various image distortions. Second, we assess robustness against embedding attacks. Third, we examine performance under noising and denoising processes. Finally, we apply state-of-the-art generative models to manipulate the watermarked images and evaluate whether the decoder can reliably extract the embedded watermarks. Experimental results show that our proposed method consistently enhances the robustness of existing post-processing watermarking models across diverse attack scenarios. Furthermore, we apply the enhanced post-processing model to strengthen the robustness of the in-processing watermarking method.

Limitations. Since our method employs both Transformer and CNN attack networks to simulate diverse distortions, the computational cost is higher than that of previous approaches that rely solely on CNNs or noise layers. Moreover, although the artifacts in watermarked images generated by our model are not very noticeable, the perceptual metrics such as PSNR and SSIM remain relatively low, leaving room for improvement.

ACKNOWLEDGMENTS

This research is supported by National Science and Technology Council, Taiwan (R.O.C), under the grant number of NSTC-114-2634-F-001-001-MBK, NSTC-113-2634-F-002-007, and NSTC-112-2222-E-001-001-MY2 and Academia Sinica under the grant number of AS-CDA-110-M09 and AS-IAIA-114-M08. We thank to National Center for High-performance Computing (NCHC) of National Institutes of Applied Research (NIAR) in Taiwan for providing computational and storage resources.

REFERENCES

- [1] Kristy Choi, Kedar Tatwawadi, Tsachy Weissman, and Stefano Ermon., “Necst: Neural joint source-channel coding.” *International Conference on Machine Learning*, 2018

- [2] Xiyang Luo, Ruohan Zhan, Huiwen Chang, Feng Yang, and Peyman Milanfar., "Distortion agnostic deep watermarking," *Computer Vision and Pattern Recognition*, 2020
- [3] Tero Karras, Samuli Laine, Miika Aittala, Janne Hellsten, Jaakko Lehtinen, and Timo Aila., "Analyzing and Improving the Image Quality of StyleGAN," *Computer Vision and Pattern Recognition*, 2020
- [4] Tero Karras, Miika Aittala, Samuli Laine, Erik Härkönen, Janwatermarkingne Hellsten, Jaakko Lehtinen, and Timo Aila., "Alias-Free Generative Adversarial Networks," *Neural Information Processing Systems*, 2021
- [5] Ning Yu, Guilin Liu, Aysegül Dundar, Andrew Tao, Bryan Catanzaro, Larry Davis, and Mario Fritz., "Dual Contrastive Loss and Attention for GANs," *International Conference on Computer Vision*, 2021
- [6] Ning Yu, Ke Li, Peng Zhou, Jitendra Malik, Larry Davis, and Mario Fritz., "Inclusive GAN: Improving Data and Minority Coverage in Generative Models," *European Conference on Computer Vision*, 2020
- [7] Ming Tao, Hao Tang, Fei Wu, Xiao-Yuan Jing, Bing-Kun Bao, and Changsheng Xu., "DF-GAN: A Simple and Effective Baseline for Text-to-Image Synthesis," *Computer Vision and Pattern Recognition*, 2022
- [8] Yufan Zhou, Ruiyi Zhang, Changyou Chen, Chunyuan Li, Chris Tensmeyer, Tong Yu, Jiuxiang Gu, Jinhui Xu, and Tong Sun., "LAFITE: Towards Language-Free Training for Text-to-Image Generation," *Computer Vision and Pattern Recognition*, 2022
- [9] Mingku Kang, Jun-Yan Zhu, Richard Zhang, Jaesik Park, Eli Shechtman, Sylvain Paris, and Taesung Park., "Scaling up GANs for Text-to-Image Synthesis," *Computer Vision and Pattern Recognition*, 2023
- [10] Yujun Shen, Jinjin Gu, Xiaoou Tang, and Bolei Zhou., "Interpreting the Latent Space of GANs for Semantic Face Editing," *Computer Vision and Pattern Recognition*, 2020
- [11] Hamza Pehlivan, Yusuf Dalva, and Aysegül Dundar., "StyleRes: Transforming the Residuals for Real Image Editing with StyleGAN," *Computer Vision and Pattern Recognition*, 2023
- [12] Maomao Li, Ge Yuan, Cairong Wang, Zhian Liu, Yong Zhang, Yongwei Nie, Jue Wang, and Dong Xu., "E4S: Fine-grained Face Swapping via Editing With Regional GAN Inversion," *Computer Vision and Pattern Recognition*, 2023
- [13] Tero Karras, Miika Aittala, Timo Aila, and Samuli Laine., "Elucidating the Design Space of Diffusion-Based Generative Models," *Neural Information Processing Systems*, 2022
- [14] Tim Brooks, Aleksander Holynski, and Alexei A. Efros., "InstructPix2Pix: Learning to Follow Image Editing Instructions," *Computer Vision and Pattern Recognition*, 2023
- [15] Alex Nichol, Prafulla Dhariwal, Aditya Ramesh, Pranav Shyam, Pamela Mishkin, Bob McGrew, Ilya Sutskever, and Mark Chen., "GLIDE: Towards Photorealistic Image Generation and Editing with Text-Guided Diffusion Models," *International Conference on Machine Learning*, 2022
- [16] Lvmin Zhang, Anyi Rao, and Maneesh Agrawala., "Adding Conditional Control to Text-to-Image Diffusion Models," *International Conference on Machine Learning*, 2023
- [17] Jiren Zhu, Russell Kaplan, Justin Johnson, and Li Fei-Fei., "Hidden: Hiding data with deep networks," *European Conference on Computer Vision*, 2018
- [18] Bang An, Mucong Ding, Tahseen Rabbani, Aakriti Agrawal, Yuancheng Xu, Chenghao Deng, Sicheng Zhu, Abdirisak Mohamed, Yuxin Wen, Tom Goldstein, and Furong Huang., "WAVES: Benchmarking the Robustness of Image Watermarks," *International Conference on Machine Learning*, 2024
- [19] Matthew Tancik, Ben Mildenhall, and Ren Ng., "StegaStamp: Invisible Hyperlinks in Physical Photographs," *Computer Vision and Pattern Recognition*, 2020
- [20] Pierre Fernandez, Guillaume Couairon, Hervé Jégou, Matthijs Douze, and Teddy Furon., "The Stable Signature: Rooting Watermarks in Latent Diffusion Models," *International Conference on Computer Vision*, 2023
- [21] Junxiong Lu, Jiangqun Ni, Wenkang Su, and Hao Xie., "Wavelet-Based CNN for Robust and High-Capacity Image Watermarking," *IEEE International Conference on Multimedia and Expo*, 2022
- [22] Ning Yu, Vladislav Skripniuk, Sahar Abdelnabi, and Mario Fritz., "Artificial Fingerprinting for Generative Models: Rooting Deepfake Attribution in Training Data," *Computer Vision and Pattern Recognition*, 2021
- [23] Yunqing Zhao, Tianyu Pang, Chao Du, Xiao Yang, Ngai-Man Cheung, and Min Lin., "A Recipe for Watermarking Diffusion Models," *arXiv preprint*, 2023
- [24] Robin Rombach, Andreas Blattmann, Dominik Lorenz, Patrick Esser, and Björn Ommer., "High-Resolution Image Synthesis with Latent Diffusion Models," *Computer Vision and Pattern Recognition*, 2022
- [25] Yuxin Wen, John Kirchenbauer, Jonas Geiping, and Tom Goldstein., "Tree-Ring Watermarks: Fingerprints for Diffusion Images that are Invisible and Robust," *Neural Information Processing Systems*, 2023
- [26] Changhoon Kim, Kyle Min, Maitreya Patel, Sheng Cheng, and Yezhou Yang., "WOUAF: Weight Modulation for User Attribution and Fingerprinting in Text-to-Image Diffusion Models," *Computer Vision and Pattern Recognition*, 2024
- [27] Nils Lukas and Florian Kerschbaum., "PTW: Pivotal Tuning Watermarking for Pre-Trained Image Generators," *USENIX: The Advanced Computing Systems Association*, 2023
- [28] Alexey Dosovitskiy, Lucas Beyer, Alexander Kolesnikov, Dirk Weissenborn, Xi-aohua Zhai, Thomas Unterthiner, Mostafa Dehghani, Matthias Minderer, Georg Heigold, Sylvain Gelly, Jakob Uszkoreit, and Neil Houlsby., "An Image is Worth 16x16 Words: Transformers for Image Recognition at Scale," *International Conference on Learning Representations*, 2021
- [29] Maithra Raghu, Thomas Unterthiner, Simon Kornblith, Chiyuan Zhang, and Alexey Dosovitskiy., "Do Vision Transformers See Like Convolutional Neural Networks?," *Neural Information Processing Systems*, 2021
- [30] Ziwei Liu, Ping Luo, Xiaogang Wang, and Xiaoou Tang., "Deep Learning Face Attributes in the Wild," *International Conference on Computer Vision*, 2015
- [31] Tsung-Yi Lin, Michael Maire, Serge Belongie, Lubomir Bourdev, Ross Girshick, James Hays, Pietro Perona, Deva Ramanan, C. Lawrence Zitnick, and Piotr Dollár., "Microsoft COCO: Common Objects in Context," *European Conference on Computer Vision*, 2014
- [32] Han Fang, Zhaoyang Jia, Hang Zhou, Zehua Ma, and Weiming Zhang., "Encoded Feature Enhancement in Watermarking Network for Distortion in Real Scenes," *IEEE TRANSACTIONS on MULTIMEDIA*, 2023
- [33] Chuan Qin, Xiaomeng Li, Zhenyi Zhang, Fengyong Li, Xinpeng Zhang, and Guorui Feng., "Print-Camera Resistant Image Watermarking With Deep Noise Simulation and Constrained Learning," *IEEE TRANSACTIONS on MULTIMEDIA*, 2024
- [34] Aleksander Madry, Aleksandar Makelov, Ludwig Schmidt, Dimitris Tsipras, and Adrian Vladu., "Towards Deep Learning Models Resistant to Adversarial Attacks," *International Conference on Learning Representations*, 2018
- [35] Kaiming He, Xiangyu Zhang, Shaoqing Ren, and Jian Sun., "Deep Residual Learning for Image Recognition," *Computer Vision and Pattern Recognition*, 2016
- [36] Alec Radford, Jong Wook Kim, Chris Hallacy, Aditya Ramesh, Gabriel Goh, Sandhini Agarwal, Girish Sastry, Amanda Askell, Pamela Mishkin, Jack Clark, Gretchen Krueger, and Ilya Sutskever., "Learning Transferable Visual Models From Natural Language Supervision," *International Conference on Machine Learning*, 2021
- [37] Dustin Podell, Zion English, Kyle Lacey, Andreas Blattmann, Tim Dockhorn, Jonas Müller, Joe Penna, and Robin Rombach., "SDXL: Improving Latent Diffusion Models for High-Resolution Image Synthesis," *arXiv preprint arXiv*, 2023
- [38] Mehrdad Saberi, Vinu Sankar Sadasivan, Keivan Rezaei, Aounon Kumar, Atoosa Chegini, Wenxiao Wang, and Soheil Feizi., "Robustness of AI-Image Detectors: Fundamental Limits and Practical Attacks," *International Conference on Learning Representations*, 2023
- [39] Jinkun You, and Yicong Zhou., "Two-Stage Watermark Removal Framework for Spread Spectrum Watermarking," *IEEE TRANSACTIONS on MULTIMEDIA*, 2024
- [40] Mingze He, Hongxia Wang, Fei Zhang, and Yuyuan Xiang., "Exploring Accurate Invariants on Polar Harmonic Fourier Moments in Polar Coordinates for Robust Image Watermarking," *IEEE TRANSACTIONS on MULTIMEDIA*, 2023
- [41] Han Fang, Zhaoyang Jia, Yupeng Qiu, Jiyi Zhang, Weiming Zhang, and Ee-Chien Chang., "De-END: Decoder-Driven Watermarking Network," *IEEE TRANSACTIONS on MULTIMEDIA*, 2023
- [42] Jinkun You, Yuan-Gen Wang, Guopu Zhu, Ligang Wu, Hongli Zhang, and Sam Kwong., "Estimating the Secret Key of Spread Spectrum Watermarking Based on Equivalent Keys," *IEEE TRANSACTIONS on MULTIMEDIA*, 2023
- [43] Yu-Feng Chen, Tzuhsuan Huang, Pin-Yen Chiu, and Jun-Cheng Chen., "Invisible Backdoor Triggers in Image Editing Model via Deep Watermarking," *arXiv preprint arXiv:2506.04879*, 2025
- [44] Jia, Shuai and Ma, Chao and Yao, Taiping and Yin, Bangjie and Ding, Shouhong and Yang, Xiaokang., "Exploring Frequency Adversarial Attacks for Face Forgery Detection," *Computer Vision and Pattern Recognition*, 2022
- [45] Luo, Cheng and Lin, Qinliang and Xie, Weicheng and Wu, Bizhu and Xie, Jinheng and Shen, Linlin., "Frequency-driven Imperceptible Adversarial Attack on Semantic Similarity," *Computer Vision and Pattern Recognition*, 2022